

---

S.M. PEREPELYTSYA, S.N. VOLKOV

Bogolyubov Institute for Theoretical Physics, Nat. Acad. of Sci. of Ukraine  
(14b, Metrolohichna Str., Kyiv 03680, Ukraine; e-mail: perepelytsya@bitp.kiev.ua;  
snvolkov@bitp.kiev.ua)

PACS 87.14.Gg, 87.15.-v,  
87.15.He

## DYNAMICS OF ION-PHOSPHATE LATTICE OF DNA IN LEFT-HANDED DOUBLE HELIX FORM

---

*The conformational vibrations of Z-DNA with counterions are studied in the framework of a phenomenological model developed. The structure of a left-handed double helix with counterions neutralizing the negatively charged phosphate groups of DNA is considered as an ion-phosphate lattice. The frequencies and the Raman intensities for the modes of Z-DNA with Na<sup>+</sup> and Mg<sup>2+</sup> ions are calculated, and the low-frequency Raman spectra are built. At the spectral interval about the frequency 150 cm<sup>-1</sup>, a new mode of ion-phosphate vibrations, which characterizes the vibrations of Mg<sup>2+</sup> counterions, is found. The results of our calculations show that the intensities of Z-DNA modes are sensitive to the concentration of magnesium counterions. The obtained results describe well the experimental Raman spectra of Z-DNA.*

*Keywords:* left-handed double helix, ion-phosphate lattice, DNA.

### 1. Introduction

DNA is a macromolecule with the double helix structure, which can adopt different forms as a response to changes of environmental conditions [1–5]. Under the natural conditions, the double helix is right-handed due to the stabilization by metal ions (counterions) that neutralize the negatively charged phosphate groups of the macromolecule backbone. As the concentration of counterions increases, the double helix can take the left-handed conformation with the zigzag-like backbone (Z-form), which is significant in many biological processes [6]. The study of the counterion influence on the structure and the dynamics of the left-handed form of a double helix is important for the understanding of the mechanisms of DNA biological functioning.

The counterions of different types can be localized in different ways with respect to the double helix phosphate groups. The experimental data for solid samples of DNA show that monovalent counterions are usually localized near the oxygen atoms of phos-

phate groups outside the macromolecule [7, 8], while the counterions of higher charge can neutralize the phosphate groups of different DNA strands or bind to the nucleic bases [9]. In a solution, the counterions have no defined positions, and they form a shell near the DNA surface [10–13]. In experiments, this shell is observed as a cloud around the double helix [14–17]. The molecular dynamics simulations of DNA counterions in a water solution show that the residence time of counterions near a phosphate group of the DNA backbone is about 1 ns [18, 19]. On this time scale, the counterions can form a regular structure around the double helix. Such structure of counterions and DNA phosphate groups may be considered as a lattice of the ionic type (ion-phosphate lattice).

The DNA ion-phosphate lattice is expected to have properties of ionic crystals. Therefore, it should be characterized by counterion vibrations with respect to the phosphate groups (ion-phosphate vibrations). The ion-phosphate vibrations must be coupled with the internal vibrations of the double helix, since the dynamics of the ion-phosphate lattice is a part of the DNA conformational dynamics. The determination

of DNA ion-phosphate modes is of paramount importance for the understanding of the counterion influence on the structure and the dynamics of a DNA double helix.

The DNA ion-phosphate vibrations may be observed in the low-frequency spectra ( $10 \div 200 \text{ cm}^{-1}$ ), where the ion vibrations in ionic crystals and electrolyte solutions are prominent [20, 21]. In this spectral interval, the modes of DNA conformational vibrations, which are characterized by the displacements of atomic groups in the nucleotide pairs (phosphates, nucleosides and nucleic bases) from their equilibrium positions, were also observed [22–29]. The conformational vibrations of the right-handed forms of a double helix are described well within the framework of the phenomenological approach [26–29]. In our previous works [30–35], this approach was extended to the case of vibrations of the monovalent counterions with respect to the phosphate groups, and the ion-phosphate vibrations were determined for the right-handed double helix with  $\text{Na}^+$ ,  $\text{K}^+$ ,  $\text{Rb}^+$ , and  $\text{Cs}^+$  counterions. The results showed that the frequencies of ion-phosphate vibrations decrease, as the counterion mass increases, from 180 to  $90 \text{ cm}^{-1}$ . The character of DNA conformational vibrations is found to be very sensitive to the counterion type and the localization with respect to the double helix atomic groups [34, 35].

In the case of *Z*-DNA, the character of conformational vibrations can be essentially different, because the structure of a left-handed double helix has the unique features. The phosphate groups of the left-handed double helix form a backbone of the zigzag shape and the nearest base pairs have different overlapping. Therefore, the nucleotide pairs form the dimers which are the elementary units of *Z*-DNA [1]. The overlapping of the base pairs inside a dimer is stronger than between dimers. At the same time, the dimeric structure of *Z*-DNA is also stabilized by counterions (usually  $\text{Mg}^{2+}$ ) that can be localized between phosphate groups of different strands of the double helix. The formation of dimers by nucleotide pairs and the localization of counterions in the DNA minor groove can be essential for the low-frequency modes of *Z*-DNA. The experimental data show that, in the low-frequency spectra of *Z*-DNA, new modes near 150 and  $42 \text{ cm}^{-1}$  are observed [36]. The origin of these modes is not determined yet. To describe the low-frequency spectra of *Z*-DNA, the approach [30–

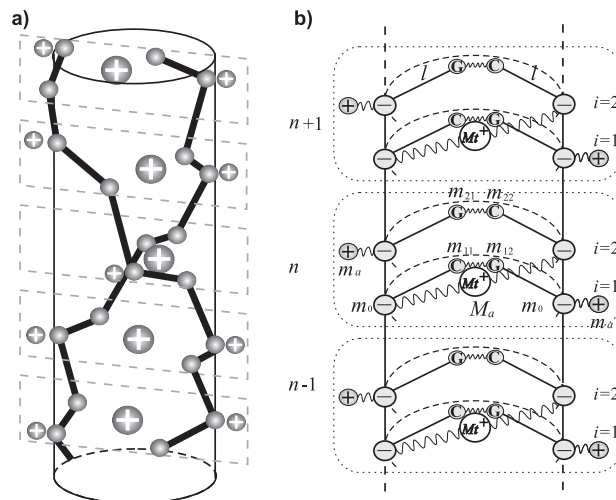


**Fig. 1.** Ion-phosphate lattices of *Z*-DNA. Zigzag-like shape of *Z*-DNA backbone (a). Model for conformational vibrations of the left-handed double helix with counterions (b). The monomer links of the model consisted of two nucleotide pairs (dimers) are shown by dotted frame

35] should be extended, by considering the features of the structure of the zigzag-like form of a double helix and the possible cases of counterion localization with respect to the phosphate groups.

The goal of the present work is to find the modes of the optic type for *Z*-DNA with counterions and to describe the conformational dynamics of the left-handed double helix. To solve this problem, the approach to the description of the dynamics of the DNA ion-phosphate lattice [30–35] is generalized in Section 2 for the case of *Z*-DNA. In Section 3, the frequencies and the Raman intensities of the modes of DNA conformational vibrations are calculated, and the low-frequency spectrum of *Z*-DNA is built. Using the calculated spectrum, the origin of new modes of *Z*-DNA observed in the experimental spectra is determined.

## 2. Model for Conformational Vibrations of the Ion-Phosphate Lattice of *Z*-DNA

To describe the conformational dynamics of the DNA ion-phosphate lattice, the typical cases of counterion localization with respect to the phosphate groups should be considered. As usual, the monovalent counterions are localized outside the double helix, where one monovalent counterion neutralizes one phosphate group (single-stranded position of counterion). At the same time, due to the zigzag-like shape of the

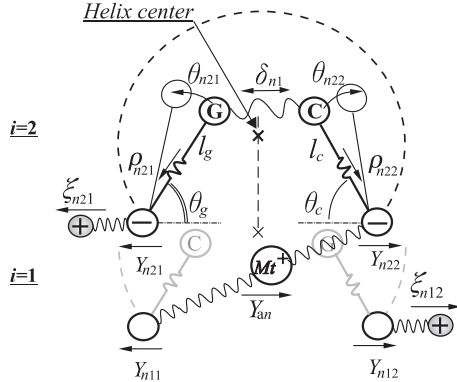


**Fig. 2.** Monomer link of the left-handed double helices (dimer of nucleotide pairs).  $l$  is the reduced length of a pendulum-nucleoside;  $\theta_0$  is the equilibrium angle;  $m$ ,  $m_0$ , and  $m_a$  are masses of nucleosides, phosphate groups, and counterions, respectively;  $X$ ,  $Y$ ,  $\theta$ ,  $\rho$ , and  $\xi$  are vibrational coordinates of the model (see the text). The arrows indicate positive directions of displacements

backbone of Z-DNA (Fig. 1, *a*), the distance between phosphate groups of different strands is rather short, which allows the localization of counterions in the minor groove of the left-handed double helix between phosphates of different strands (cross-stranded position of a counterion). The cross-stranded position is more favorable for bivalent counterions (Fig. 1, *a*).

To describe the conformational vibrations of a DNA double helix, the phenomenological approach [26–28] is used. In the framework of this approach, the phosphate groups ( $\text{PO}_4 + \text{C}_{5'}$ ) and the nucleosides are modeled as masses  $m_0$  and  $m$ , respectively. The nucleosides rotate as physical pendulums with respect to the phosphate groups in plane of nucleotide pair. The physical pendulums are characterized by reduced length  $l$ . The nucleosides of different chains are paired by H-bonds (Fig. 1, *b*). The motions of structural elements of a monomer link are considered in the plane orthogonal to the helical axis (transverse vibrations). The longitudinal vibrations of the macromolecule atomic groups have much higher frequencies and are beyond the scope of this work.

According to the dimeric structure of the zigzag-like double helix, the monomer link of the model of Z-DNA consists of two nucleotide pairs. The nucleosides in a dimer have usually an alternating sequence of guanine (G) and cytosine (C) nucleic bases [1]. The displacements of nucleosides and phosphate groups in a DNA monomer link are described by coor-

dinate  $Y$ . The coordinate  $\theta$  describes the deviations of pendulum-nucleosides from their equilibrium positions (angle  $\theta_0$ ) in the plane of the complementary DNA pair. The vibrations of a deoxyribose and a base with respect to each other, inside the nucleoside (intranucleoside mobility), are described by changes of pendulum lengths  $\rho$ . The vibrations of a counterion in single-stranded positions are described by the coordinate  $\xi$ . For description of vibrations of a counterion in cross-stranded positions, the coordinate  $Y_a$  is used. The vibrational coordinates of the model and the positive directions of displacements are showed on Fig. 2.

Within the framework of the introduced model of DNA ion-phosphate lattice dynamics, the energy of vibrations of structural elements of the double helix can be written as follows:

$$E = \sum_n (K_n + U_n + U_{n,n-1}), \quad (1)$$

where  $K_n$  and  $U_n$  are the kinetic and potential energies of the monomer link  $n$  of the DNA ion-phosphate lattice,  $U_{n,n-1}$  is the potential energy of interaction along the chain. The kinetic energy of the monomer link can be written as

$$K_n = K_{0n} + K_{an}, \quad (2)$$

where  $K_{0n}$  and  $K_{an}$  are the energies of vibrations of structure elements in nucleotide pairs of the  $n$ -th dimer and counterions, respectively. The potential energy of displacements of the masses in the monomer link can be written down in the form

$$U_n = U_{0n} + U_{an}, \quad (3)$$

where  $U_{0n}$  and  $U_{an}$  are the energies of vibrations of the masses in nucleotide pairs of a dimer and the energy of vibrations of counterions, respectively.

The expressions for  $K_{0n}$  and  $U_{0n}$  for Z-DNA can be written in the form

$$K_{0n} = \frac{1}{2} \sum_i^2 \sum_j^2 [M_{ij} \dot{Y}_{nij}^2 + m_{ij} (\dot{\rho}_{nij}^2 + l_{ij}^2 \dot{\theta}_{nij}^2 + 2l_{ij}^s \dot{\theta}_{nij} \dot{Y}_{nij} + 2b_{ij} \dot{\rho}_{nij} \dot{Y}_{nij})], \quad (4)$$

$$U_{0n} = \frac{1}{2} \sum_i^2 [\alpha \delta_{ni}^2 + \sum_j^2 (\sigma_{ij} \rho_{nij}^2 + \beta_{ij} \theta_{nij}^2)] + \frac{1}{2} \sum_j^2 [g_\theta (\theta_{n1j} - \theta_{n2j})^2 + g_\rho (\rho_{n1j} - \rho_{n2j})^2 + g_y (Y_{n1j} - Y_{n2j})^2], \quad (5)$$

where  $l_{ij}^s = l_{ij}a_{ij}$ ;  $a_{ij} = \sin \theta_{0ij}$ ;  $b_{ij} = \cos \theta_{0ij}$ ;  $n$  enumerates the dimers of a macromolecule;  $i = 1, 2$  enumerates the nucleotide pairs in these dimers;  $j = 1, 2$  enumerates the chains of the double helix;  $\alpha$ ,  $\sigma_{ij}$ , and  $\beta_{ij}$  are the force constants describing the H-bond stretching in base pairs, intranucleoside mobility, and rotation of nucleosides with respect to the backbone chain in the base-pair plane, respectively;  $g_\theta$ ,  $g_\rho$ , and  $g_y$  are the force constants describing the interaction of nucleic bases and the interaction between phosphate groups of different nucleotide pairs in dimers. The variable  $\delta_{ni}$  describes the stretching of H-bonds in the base pairs (Fig. 2). In the present work, it is determined analogically to [27, 28]:  $\delta_{ni} \approx l_{si1}\theta_{ni1} + l_{si2}\theta_{ni2} + Y_{ni1} + Y_{ni2} + b_{i1}\rho_{ni1} + b_{i2}\rho_{ni2}$ .

The kinetic and potential energies of counterion vibrations in the ion-phosphate lattice of Z-DNA can be written as follows:

$$K_{an} = \frac{m_a}{2} [(\dot{Y}_{n21} + \dot{\xi}_{n21})^2 + (\dot{Y}_{n12} + \dot{\xi}_{n12})^2] + \frac{M_a}{2} \dot{Y}_{an}^2, \quad (6)$$

$$U_{an} = \frac{\gamma}{2} (\xi_{n21}^2 + \xi_{n12}^2) + \frac{\gamma_a}{2} [(Y_{an} - Y_{n22})^2 + (Y_{an} + Y_{n11})^2], \quad (7)$$

where  $\gamma$  and  $\gamma_a$  are the force constants for the counterions in single-stranded and cross-stranded positions, respectively;  $m_a$  and  $M_a$  are the masses of counterions in single-stranded and cross-stranded positions. In relations (6) and (7), the first terms describe the kinetic and potential energies of vibrations of counterions in single-stranded positions, while the last terms describe the kinetic and potential energies of vibrations of counterions in cross-stranded positions.

To describe the low-frequency Raman spectra of Z-DNA, we intend to find the optic-type phonons, which are observed in the experimental spectra from 10 to 200  $\text{cm}^{-1}$ . Therefore, we will consider the modes characterizing the vibrations of DNA atomic groups inside the Z-DNA monomers (dimers of nucleotide pairs) which are prominent in the considered spectral interval. The vibrations of the pair dimers with respect to one another occur, by our estimations, with essentially lower frequencies ( $< 5 \text{ cm}^{-1}$ ). Since only the long-range optic vibrations are observed in the low-frequency Raman spectra, we will consider the limited long-wave ( $\bar{k} \rightarrow 0$ ) vibrational modes of the ion-phosphate lattice in Z-DNA. From the point of

the theory of lattice vibrations, such approximation is the same as the neglect of the interaction along a chain [37]. Therefore, we omit the interaction term:  $U_{n,n-1} \approx 0$ . Within this approximation, the equations of motions take the form

$$\frac{d}{dt} \frac{\partial K_{0n}}{\partial \dot{q}_n} + \frac{d}{dt} \frac{\partial K_{an}}{\partial \dot{q}_n} - \frac{\partial U_{0n}}{\partial q_n} - \frac{\partial U_{an}}{\partial q_n} = 0, \quad (8)$$

where  $q_n$  denotes some vibrational coordinate in a monomer link of the model (Fig. 2). The equations of motion (8) in explicit form for the model coordinates of a Z-DNA double helix are shown in Appendix.

To estimate the frequencies of Z-DNA conformational vibrations, we used the same force constants  $\alpha = 85 \text{ kcal/mol}\text{\AA}^2$ ,  $\beta = 40(46) \text{ kcal/mol}$ , and  $\sigma = 43(22) \text{ kcal/mol}\text{\AA}^2$  as in B(A)-DNA [26, 27]. The values of  $\beta$  and  $\sigma$  in the case of a left-handed Z-DNA are different for G and C nucleosides, and they are taken to be the same as in A- and B-forms, respectively. The constants  $g_\theta$  and  $g_\rho$  are equal to 20 kcal/mol, while the constant  $g_y = 8 \text{ kcal/mol}\text{\AA}^2$ , [26, 27]. The structure parameters of the model ( $l$  and  $\theta_0$ ) for Z-DNA are determined, by using X-ray data (pdb code: 1dcg) [38].

The constants of ion-phosphate vibrations have been determined in our previous works [31, 35], by using the theory of ionic crystals. It has been shown that the constant of ion-phosphate vibrations depends mostly on the dielectric constant of a DNA ion-hydrate shell, the Madelung constant of the system describing the electrostatic interaction of an ion with all charges of the system, and parameters of the ion (Pauling radii of a cation and an oxygen atom). The dielectric constant has been determined, by considering the properties of the hydration shell of DNA with the counterions of different types. The Madelung constant has been calculated from the structure of a double helix. As a result, the values of  $\gamma$  and  $\gamma_a$  constants have been calculated for the ion-phosphate lattice of DNA with alkali metal counterions in the single-stranded position and for magnesium counterions in the cross-stranded position. The magnesium counterions are considered with the hydration shell, because the size of a hydrated  $\text{Mg}^{2+}$  ion corresponds to the distances between phosphate groups of the left-handed double helix. The hydration shell of a magnesium ion consists of 4 water molecules that are strongly bound with the ion [39]. Thus, the constants of ion-phosphate vibrations have the following values:

$\gamma = 52 \text{ kcal/mol\AA}^2$  in the case of  $\text{Na}^+$  counterions [31], while  $\gamma_a = 62 \text{ kcal/mol\AA}^2$  [35] in the case of  $\text{Mg}^{2+}$ . Using such parameters, the frequencies of *Z*-DNA conformational vibrations are estimated by the formulae (1)–(8).

### 3. Low-Frequency Raman Spectra of *Z*-DNA

According to the character of vibrations of structural elements in DNA nucleotide pairs, the obtained modes can be classified as the modes of ion-phosphate vibrations (**Ion**), H-bond stretching modes (**H**), modes of intranucleoside vibrations (**S**), and modes of backbone vibrations (**B**). To characterize the influence of counterion mobility, the frequencies of *Z*-DNA conformational vibrations for the dimers without  $\text{Mg}^{2+}$  counterions are also calculated. The frequencies of *Z*-DNA conformational vibrations are presented in the Table.

The calculations show that the frequencies of ion-phosphate vibrations depend on the counterion posi-

**Frequencies of *Z*-DNA conformational vibrations ( $\text{cm}^{-1}$ ). The results for two cases are shown: *Z*-DNA with  $\text{Na}^+$  and  $\text{Mg}^{2+}$  counterions, and *Z*-DNA with  $\text{Na}^+$  counterions only. The calculated frequencies are compared with the experimental data for *Z*-DNA [23, 36] and with the calculation data for *B*-DNA [31]**

Mode	<i>Z</i> -DNA				<i>B</i> -DNA	
	Theory		Experiment*		Theory [31] ( $\text{Na}^+$ )	
	( $\text{Na}^+$ , $\text{Mg}^{2+}$ )	( $\text{Na}^+$ )	[36]	[23]		
<b>Ion</b>	$\omega_{\text{Ion1}}$	180	180	–	–	181
	$\omega_{\text{Ion2}}$	180	180	–	–	181
	$\omega_{\text{Ion3}}$	152	–	153w	–	–
<b>H</b>	$\omega_{\text{H1}}$	110	107	112s	116sh	110
	$\omega_{\text{H2}}$	106	106	–	100	–
	$\omega_{\text{H3}}$	96	68	–	–	–
	$\omega_{\text{H4}}$	59	66	70	66	58
<b>S</b>	$\omega_{\text{S1}}$	45	45	45vw	–	79
	$\omega_{\text{S2}}$	44	41	–	–	–
	$\omega_{\text{S3}}$	40	28	–	–	–
<b>B</b>	$\omega_{\text{B1}}$	25	25	25	–	16
	$\omega_{\text{B2}}$	20	20	–	–	14
	$\omega_{\text{B3}}$	11	11	–	–	–
	$\omega_{\text{B4}}$	11	11	–	–	–

\*s – strong, sh – shoulder, w – weak, vw – very weak.

tion. In the case of  $\text{Na}^+$  counterions in the single-stranded position, there are two degenerate modes ( $\omega_{\text{Ion1}}$  and  $\omega_{\text{Ion2}}$ ) with the frequencies at the top of the DNA low-frequency spectrum (near  $180 \text{ cm}^{-1}$ ). These modes are characteristic of the both right- and left-handed double helix forms. The vibrations of hydrated  $\text{Mg}^{2+}$  ions in the cross-stranded position ( $\omega_{\text{Ion3}}$ ) have an essentially lower frequency, which is due to the big size and big mass of a hydrated  $\text{Mg}^{2+}$  ion ( $M_a = 96 \text{ a.u.m.}$ ). The vibrations of a  $\text{Mg}^{2+}$  counterion in the cross-stranded position do not influence the vibrations of  $\text{Na}^+$  counterions outside the double helix.

The H-bond stretching in the nucleotide pairs of *Z*-DNA is characterized by 4 modes ( $\omega_{\text{H1}}$ ,  $\omega_{\text{H2}}$ ,  $\omega_{\text{H3}}$ , and  $\omega_{\text{H4}}$ ); while, in the case of the right-handed form of a double helix, there are only two modes. Two additional modes of H-bond stretching,  $\omega_{\text{H2}}$  and  $\omega_{\text{H3}}$ , appear due to the formation of dimers of nucleotide pairs in the *Z*-DNA structure. The modes  $\omega_{\text{H1}}$  and  $\omega_{\text{H2}}$  have practically the same frequency for *B*- and *Z*-DNA. The modes  $\omega_{\text{H3}}$  and  $\omega_{\text{H4}}$  of *Z*-DNA are sensitive to a  $\text{Mg}^{2+}$  counterion in the cross-stranded position.

In the case of a left-handed double helix, there are 3 modes of intranucleoside vibrations  $\omega_{\text{S1}}$ ,  $\omega_{\text{S2}}$ , and  $\omega_{\text{S3}}$  with rather close frequency values (about  $45 \text{ cm}^{-1}$ ). The modes of intranucleoside vibrations depend essentially on the double helix form. In the case of *B*-DNA, there is only one mode of intranucleoside vibrations  $\omega_{\text{S1}}$ , which has an essentially higher frequency than the respective modes of *Z*-DNA. The mode  $\omega_{\text{S3}}$  shifts to lower frequencies if there is no  $\text{Mg}^{2+}$  counterion in the cross-stranded position.

The modes of backbone vibrations ( $\omega_{\text{B1}}$ ,  $\omega_{\text{B2}}$ ,  $\omega_{\text{B3}}$ , and  $\omega_{\text{B4}}$ ) are the lowest in the DNA low-frequency spectrum. In the case of the ion-phosphate lattice of *Z*-DNA, there are two modes ( $\omega_{\text{B1}}$  and  $\omega_{\text{B2}}$ ) near  $25 \text{ cm}^{-1}$  and two modes ( $\omega_{\text{B3}}$  and  $\omega_{\text{B4}}$ ) with close frequency values (about  $10 \text{ cm}^{-1}$ ). In the case of the ion-phosphate lattice of *B*-DNA, there are only two modes  $\omega_{\text{B1}}$  and  $\omega_{\text{B2}}$  with close frequency values. This difference of *B*- and *Z*-DNA spectra is a manifestation of the dimeric structure of the left-handed structure of the DNA double helix.

To compare our calculations with the experimental spectra, the Raman intensities are calculated with the use of the approach developed in [34, 35]. As a result, the low-frequency Raman spectra of DNA in the *Z*-

form of the double helix are built for different degrees of filling ( $P$ ) of the ion-phosphate lattice by  $\text{Mg}^{2+}$  counterions (Fig. 3). The parameter  $P$  equals 1 if all dimers of Z-DNA contain  $\text{Mg}^{2+}$  counterions, and  $P$  equals 0 if there is no counterions in dimers. The mode intensities are normalized to the intensity of the mode  $\omega_{\text{H1}}$ . The half-width of spectral lines is considered to be equal to  $5 \text{ cm}^{-1}$ .

The obtained spectrum is divided into four intervals with similar intensities of the modes of DNA conformational vibrations (Fig. 3, *a-d*). The interval  $(0 \div 40) \text{ cm}^{-1}$  (Fig. 3, *a*) is characterized by the modes of backbone vibrations (**B**). These modes are the most intense in the DNA low-frequency spectrum, because their energy is lower than  $k_{\text{B}}T$  at room temperature. Due to the high intensity, the modes of backbone vibrations are observed in the experimental spectrum as a peak near  $25 \text{ cm}^{-1}$  [36]. As the filling of the ion-phosphate lattice by  $\text{Mg}^{2+}$  counterions in the dimers increases, the intensity of this band decreases.

In the frequency interval  $(40 \div 60) \text{ cm}^{-1}$  (Fig. 3, *b*), there is a band characterizing the intranucleoside vibrations (**S**). The intensity of this band is essentially lower than that of **B** band formed by modes of backbone vibrations. Therefore, in the experimental spectrum [36], **S** band is observed as a weak mode near  $45 \text{ cm}^{-1}$ . The dependence of the intensity of this band on the filling parameter  $P$  is weak.

The frequency interval  $(60 \div 130) \text{ cm}^{-1}$  (Fig. 3, *c*) is characterized by two bands at  $70$  and  $110 \text{ cm}^{-1}$ , which are caused by the modes of H-bond stretching in the base pairs (**H**). The intensity of the  $70\text{-cm}^{-1}$  band decreases, as the filling of the ion-phosphate lattice by  $\text{Mg}^{2+}$  counterions increases, while the intensity of the  $110\text{-cm}^{-1}$  band remains the same. The comparison of the calculated spectra (Fig. 3, *c*) with the experimental Raman spectra [23, 36] shows that, at these frequencies, there are two strong modes. The frequency and the intensity of the observed modes agree with the results of our calculations.

In the spectral interval  $(130 \div 200) \text{ cm}^{-1}$  (Fig. 3, *d*), there are two bands at  $150$  and  $180 \text{ cm}^{-1}$  characterizing the ion-phosphate vibrations of  $\text{Mg}^{2+}$  and  $\text{Na}^+$  counterions, respectively (**Ion**). The dependence of intensity on the filling parameter  $P$  is essential only for the mode of ion-phosphate vibrations of  $\text{Mg}^{2+}$  counterions. The comparison with

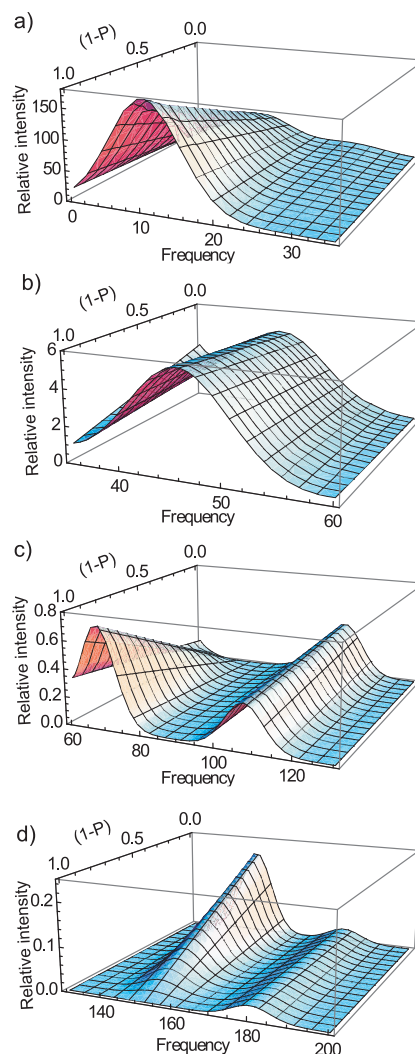


**Fig. 3.** Low-frequency Raman spectra of Z-DNA with different fillings of the ion-phosphate lattice by  $\text{Mg}^{2+}$  counterions. *a*) Backbone vibrations interval  $(0 \div 40) \text{ cm}^{-1}$  (**B**). *b*) Intranucleoside vibrations interval  $(40 \div 60) \text{ cm}^{-1}$  (**S**). *c*) H-bond stretching vibrations interval  $(60 \div 130) \text{ cm}^{-1}$  (**H**). *d*) Ion-phosphate vibrations interval  $(130 \div 200) \text{ cm}^{-1}$  (**Ion**)

the experimental spectrum shows that, in the Raman spectrum of Z-DNA, a very weak mode near  $153 \text{ cm}^{-1}$  is observed [36] that corresponds to the calculated  $150\text{-cm}^{-1}$  band. The vibrations of  $\text{Na}^+$  counterions are not observed in the low-frequency spectrum of Z-DNA. However, in the spectra of dry DNA films, the mode resembling the mode of ion-phosphate vibrations has been detected [22, 25, 30, 31].

#### 4. Conclusions

The conformational vibrations of  $Z$ -DNA are studied with regard for the double helices with counterions as a lattice of the ionic type (ion-phosphate lattice). To find the vibrational modes of the ion-phosphate lattice, a phenomenological model is developed taking the feature of a  $Z$ -DNA structure into account. In the model, the monovalent counterions are localized outside the double helix, and the bivalent counterions are localized between the phosphate groups of nucleotide dimers of  $Z$ -DNA. Using the developed model, the frequencies and the Raman intensities of vibrational modes are calculated for DNA with  $\text{Na}^+$  and  $\text{Mg}^{2+}$  counterions. The results show that the obtained frequencies of the H-bond stretching in nucleotide pairs and the frequencies of intranucleoside vibrations differ from the respective frequencies in the case of the right-handed DNA double helix. The reason for such difference is in the dimeric structure of the left-handed  $Z$ -DNA. The new mode of ion-phosphate vibrations about a frequency of  $150 \text{ cm}^{-1}$  is determined, which characterizes the vibrations of  $\text{Mg}^{2+}$  counterions. The intensity of this mode is rather large, and it is observed in the experimental Raman spectra of  $Z$ -DNA [36]. The modes of ion-phosphate vibrations in the case of  $\text{Na}^+$  counterions ( $180 \text{ cm}^{-1}$ ) are weak and do not observed experimentally. The modes of  $Z$ -DNA conformational vibrations are very sensitive to the concentration of  $\text{Mg}^{2+}$  counterions in the solution. The developed model describes the conformational vibrations of  $Z$ -DNA with  $\text{Na}^+$  and  $\text{Mg}^{2+}$  counterions and allows one to determine the origin of new modes in the experimental low-frequency Raman spectra of  $Z$ -DNA.

*The present work was partially supported by the Grant for the Young Scientists of the NAS of Ukraine 0112U005857 and by the project of the NAS of Ukraine 0110U007540.*

#### APPENDIX

##### Equations of Motion

To obtain a more convenient form of the equations of motion, the following variables are used:  $Y_c^n = Y_{11}^n + Y_{22}^n$ ,  $y_c^n = Y_{11}^n - Y_{22}^n$ ,  $\theta_c^n = \theta_{11}^n + \theta_{22}^n$ ,  $\eta_c^n = \theta_{11}^n - \theta_{22}^n$ ,  $\rho_c^n = \rho_{11}^n + \rho_{22}^n$ ,  $r_c^n = \rho_{11}^n - \rho_{22}^n$ ,  $Y_g^n = Y_{21}^n + Y_{12}^n$ ,  $y_g^n = Y_{21}^n - Y_{12}^n$ ,  $\theta_g^n = \theta_{21}^n + \theta_{12}^n$ ,  $\eta_g^n = \theta_{21}^n - \theta_{12}^n$ ,  $\rho_g^n = \rho_{21}^n + \rho_{12}^n$ ,  $r_g^n = \rho_{21}^n - \rho_{12}^n$ ,  $\xi_1^n = \xi_{21}^n + \xi_{12}^n$ ,  $\xi_2^n = \xi_{21}^n - \xi_{12}^n$ . As a result, the equations of motion (8) for optic

long-wave vibrations are split into two subsystems of coupled equations:

$$\left\{ \begin{array}{l} \ddot{Y}_c^n + \frac{m_c b_c}{M_c} \rho_c^n + \frac{m_c l_c^s}{M_c} \ddot{\theta}_c^n + \frac{M_a}{M_c} \gamma_{a0} Y_c^n - g_{yc} (Y_c^n - Y_g^n) + \\ + \alpha_c (Y_g^n + Y_c^n + l_c^s \theta_g^n + l_c^s \theta_c^n + b_g \rho_g^n + b_c \rho_c^n) = 0; \\ \ddot{Y}_g^n + \frac{m_g b_g}{M_g} \rho_g^n + \frac{m_g l_g^s}{M_g} \ddot{\theta}_g^n + \frac{m_a}{M_g} (\ddot{Y}_g^n + \ddot{\xi}_1^n) - g_{yg} (Y_c^n - Y_g^n) + \\ + \alpha_g (Y_g^n + Y_c^n + l_g^s \theta_g^n + l_c^s \theta_c^n + b_g \rho_g^n + b_c \rho_c^n) = 0; \\ \ddot{\theta}_g^n + \ddot{Y}_g^n \frac{a_g}{l_g} + \beta_g \theta_g^n - g_{\theta g} (\theta_c^n - \theta_g^n) + \\ + \alpha_g \frac{M_g a_g}{m_g l_g} (Y_g^n + Y_c^n + l_c^s \theta_g^n + l_c^s \theta_c^n + b_g \rho_g^n + b_c \rho_c^n) = 0; \\ \ddot{\theta}_c^n + \ddot{Y}_c^n \frac{a_c}{l_c} + \beta_c \theta_c^n - g_{\theta c} (\theta_c^n - \theta_g^n) + \\ + \alpha_c \frac{M_c a_c}{m_c l_c} (Y_g^n + Y_c^n + l_g^s \theta_g^n + l_c^s \theta_c^n + b_g \rho_g^n + b_c \rho_c^n) = 0; \\ \ddot{\rho}_g^n + b_g \ddot{Y}_g^n + \sigma_g \rho_g^n - g_{\rho g} (\rho_c^n - \rho_g^n) + \\ + \alpha_g \frac{M_g b_g}{m_g} (Y_g^n + Y_c^n + l_g^s \theta_g^n + l_c^s \theta_c^n + b_g \rho_g^n + b_c \rho_c^n) = 0; \\ \ddot{\rho}_c^n + b_c \ddot{Y}_c^n + \sigma_c \rho_c^n - g_{\rho c} (\rho_c^n - \rho_g^n) + \\ + \alpha_c \frac{M_c b_c}{m_c} (Y_g^n + Y_c^n + l_g^s \theta_g^n + l_c^s \theta_c^n + b_g \rho_g^n + b_c \rho_c^n) = 0; \\ \ddot{Y}_g^n + \ddot{\xi}_1^n + \gamma_0 \xi_1^n = 0; \end{array} \right. \\ \\ \left\{ \begin{array}{l} \ddot{y}_c^n + \frac{m_c b_c}{M_c} \ddot{r}_c^n + \frac{m_c l_c^s}{M_c} \ddot{\eta}_c^n - \\ - \frac{M_a}{M_c} \gamma_{a0} (2y_a^n - y_c^n) + g_{yc} (y_c^n + y_g^n) + \\ + \alpha_c (y_g^n + y_c^n + l_g^s \eta_g^n + l_c^s \eta_c^n + b_g r_g^n + b_c r_c^n) = 0; \\ \ddot{y}_g^n + \frac{m_g b_g}{M_g} \ddot{r}_g^n + \frac{m_g l_g^s}{M_g} \ddot{\eta}_g^n + \frac{m_a}{M_g} (y_g^n + \xi_2^n) + g_{yg} (y_c^n + y_g^n) + \\ + \alpha_g (y_g^n + y_c^n + l_g^s \eta_g^n + l_c^s \eta_c^n + b_g r_g^n + b_c r_c^n) = 0; \\ \ddot{\eta}_g^n + \ddot{y}_g^n \frac{a_g}{l_g} + \beta_g \eta_g^n + g_{\theta g} (\eta_c^n + \eta_g^n) + \\ + \alpha_g \frac{M_g a_g}{m_g l_g} (y_g^n + y_c^n + l_g^s \eta_g^n + l_c^s \eta_c^n + b_g r_g^n + b_c r_c^n) = 0; \\ \ddot{\eta}_c^n + \ddot{y}_c^n \frac{a_c}{l_c} + \beta_c \eta_c^n + g_{\theta c} (\eta_c^n + \eta_g^n) + \\ + \alpha_c \frac{M_c a_c}{m_c l_c} (y_g^n + y_c^n + l_g^s \eta_g^n + l_c^s \eta_c^n + b_g r_g^n + b_c r_c^n) = 0; \\ \ddot{r}_g^n + b_g \ddot{y}_g^n + \sigma_g r_g^n + g_{\rho g} (r_c^n + r_g^n) + \\ + \alpha_g \frac{M_g b_g}{m_g} (y_g^n + y_c^n + l_g^s \eta_g^n + l_c^s \eta_c^n + b_g r_g^n + b_c r_c^n) = 0; \\ \ddot{r}_c^n + b_c \ddot{y}_c^n + \sigma_c r_c^n + g_{\rho c} (r_c^n + r_g^n) + \\ + \alpha_c \frac{M_c b_c}{m_c} (y_g^n + y_c^n + l_g^s \eta_g^n + l_c^s \eta_c^n + b_g r_g^n + b_c r_c^n) = 0; \\ \ddot{y}_g^n + \ddot{\xi}_2^n + \gamma_0 \xi_2^n = 0; \\ 2\ddot{y}_a^n + 2\gamma_{a0} (2Y_a^n - y_c^n) = 0, \end{array} \right.$$

where  $\alpha_g = \alpha/M_g$ ,  $\alpha_c = \alpha/M_c$ ,  $\beta_g = \beta/m_g l_g^2$ ,  $\beta_c = \beta/m_c l_c^2$ ,  $\sigma_g = \sigma/m_g$ ,  $\sigma_c = \sigma/m_c$ ,  $\gamma_0 = \gamma/m_a$ ,  $\gamma_{a0} = \gamma_a/M_a$ ,  $g_{\theta g} = g_{\theta}/m_g l_g^2$ ,  $g_{\theta c} = g_{\theta}/m_c l_c^2$ ,  $g_{\rho g} = g_{\rho}/m_g$ ,  $g_{\rho c} = g_{\rho}/m_c$ ,  $g_{yg} = g_y/m_g$ ,  $g_{yc} = g_y/m_c$ ,  $a_c = \sin \theta_{0c}$ ,  $a_g = \sin \theta_{0g}$ ,  $b_c = \cos \theta_{0c}$ ,  $b_g = \cos \theta_{0g}$ ,  $l_c^s = l_c \sin \theta_{0c}$ ,  $l_g^s = l_g \sin \theta_{0g}$ .

The first subsystem of the equations of motion describes symmetric vibrations of the nucleotides in dimers, while the

second subsystem describes antisymmetric vibrations of nucleotides. The obtained equations of motions are solved using the substitution:  $q_n = \tilde{q}_n \exp(i\omega t)$ , where  $\tilde{q}_n$  and  $\omega$  are the amplitude and the frequency for some coordinate of vibrations, respectively. As a result, the equation for frequencies of long-wave vibrations of Z-DNA is obtained. From the first subsystem of the equations of motion, the equation for frequencies  $\omega_{H1}$ ,  $\omega_{H3}$ ,  $\omega_{S2}$ ,  $\omega_{S3}$ ,  $\omega_{B2}$ ,  $\omega_{B4}$ , and  $\omega_{Ion1}$  is derived. The second subsystem of the equations of motion gives the equation for frequencies  $\omega_{H2}$ ,  $\omega_{H4}$ ,  $\omega_{S1}$ ,  $\omega_{B1}$ ,  $\omega_{B3}$ ,  $\omega_{Ion2}$ , and  $\omega_{Ion3}$ . Using the parameters discussed in Section 2, the frequencies of the modes of Z-DNA conformational vibrations are calculated numerically. The values of the calculated frequencies are showed in the Table.

- W. Saenger, *Principles of Nucleic Acid Structure* (Springer, New York, 1984).
- Yu.P. Blagoi, V.L. Galkin, G.O. Gladchenko *et al.*, *The Complexes of Nucleic Acids and Metals in Solutions* (Naukova Dumka, Kiev, 1991) (in Russian).
- V.I. Ivanov, L.E. Minchenkova, A.K. Schyolkina, and A.I. Poletayev, *Biopolymers* **12**, 89 (1973).
- V.Ya. Maleev, M.A. Semenov, A.I. Gasan, and V.A. Kashpur, *Biofizika* **38**, 768 (1993).
- L.D. Williams and L.J. Maher, *Annu. Rev. Biophys. Biomol. Struct.* **29**, 497 (2000).
- A. Rich and S. Zhang, *Nature Reviews* **4**, 566 (2003).
- V. Tereshko *et al.*, *Nucleic Acids Res.* **29**, 1208 (2001).
- V. Tereshko, G. Minasov, and M. Egli, *J. Am. Chem. Soc.* **121**, 470 (1999).
- N.V. Hud and M. Polak, *Current Opinion Struct. Biol.* **11**, 293 (2001).
- G.S. Manning, *Q. Rev. Biophys.* **11**, 179 (1978).
- M.D. Frank-Kamenetskii, V.V. Anshelevich, and A.V. Lukashin, *Sov. Phys. Usp.* **151**, 595 (1987).
- Y. Levin, *Rep. Prog. Phys.* **65**, 1577 (2002).
- A.A. Kornyshev *et al.*, *Rev. Mod. Phys.* **79**, 943 (2007).
- R. Das, T.T. Mills, L.W. Kwok *et al.*, *Phys. Rev. Lett.* **90**, 188103 (2003).
- K. Andersen, R. Das, H.Y. Park *et al.*, *Phys. Rev. Lett.* **93**, 248103 (2004).
- K. Andresen, X. Qui, S.A. Pabit *et al.*, *Biophys. J.* **95**, 287 (2008).
- X. Qiu, L.W. Kwok, H.Y. Park *et al.*, *Phys. Rev. Lett.* **101**, 228101 (2008).
- P. Varnai and K. Zakrzewska, *Nucleic Acids Res.* **32**, 4269 (2004).
- S.Y. Ponomarev, K.M. Thayer, and D.L. Beveridge, *Proc. Natl. Acad. Sci. USA* **101**, 14771 (2004).
- C. Kittel, *Introduction to Solid State Physics* (Wiley, New York, 1954).
- I.A. Heisler, K. Mazur, and S.R. Meech, *J. Phys. Chem.* **115**, 2563 (2011).
- J.W. Powell, G.S. Edwards, L. Genzel *et al.*, *Phys. Rev. A* **35**, 3929 (1987).
- O.P. Lamba, A.H.-J. Wang, and G.J. Thomas, jr., *Biopolymers* **28**, 667 (1989).
- T. Weidlich, S.M. Lindsay, Qi Rui *et al.*, *J. Biomol. Struct. Dyn.* **8**, 139 (1990).
- T. Weidlich, J.W. Powell, L. Genzel, and A. Rupprecht, *Biopolymers* **30**, 477 (1990).
- S.N. Volkov and A.M. Kosevich, *Molek. Biol.* **21**, 797 (1987).
- S.N. Volkov and A.M. Kosevich, *J. Biomol. Struct. Dyn.* **8**, 1069 (1991).
- S.N. Volkov, *Biopolymers and Cell* **7**, 40 (1991).
- A.M. Kosevich and S.N. Volkov, *Nonlinear Excitations in Biomolecules*, edited by M. Peyrard (Springer, New York, 1995), Chapter 9.
- S.M. Perepelytsya and S.N. Volkov, *Ukr. J. Phys.* **49**, 1072 (2004); arXiv: q-bio.BM/0412022.
- S.M. Perepelytsya and S.N. Volkov, *Eur. Phys. J. E* **24**, 261 (2007).
- S.M. Perepelytsya and S.N. Volkov, *Biofiz. Bull.* **23(2)**, 5 (2009); arXiv: q-bio.BM/0805.0696v1.
- S.M. Perepelytsya and S.N. Volkov, *Eur. Phys. J. E* **31**, 201 (2010).
- S.M. Perepelytsya and S.N. Volkov, *Ukr. J. Phys.* **55**, 1182 (2010).
- S.M. Perepelytsya and S.N. Volkov, *J. Molec. Liq.* **5**, 1182 (2011).
- T. Weidlich, S.M. Lindsay, W.L. Peticolas, and G.A. Thomas, *J. Biomolec. Struct. Dyn.* **7**, 849 (1990).
- A.M. Kosevich, *Theory of Crystal Lattice* (Wiley-VCH, Berlin, 1999).
- R.V. Gessner, C.A. Frederick, G.J. Quigley *et al.*, *J. Biol. Chem.* **264**, 7921 (1989).
- N.A. Izmailov, *Electrochemistry of Solutions* (Khimiya, Moscow, 1976) (in Russian).

Received 29.03.13

С.М. Перепелиця, С.Н. Волков

## ДИНАМІКА ІОН-ФОСФАТНОЇ ҐРАТКИ ДНК В ЛІВІЙ ФОРМІ ПОДВІЙНОЇ СПІРАЛІ

## Резюме

У рамках розвиненої феноменологічної моделі досліджено конформаційні коливання Z-ДНК з протиіонами. Структура лівозакрученої подвійної спіралі з протиіонами, що нейтралізують від'ємно заряджені фосфатні групи остова макромолекули, представляється у вигляді іон-фосфатної ґратки. Розраховано частоту та інтенсивності комбінаційного розсіювання світла (КРС) для мод Z-ДНК з іонами  $\text{Na}^+$  і  $\text{Mg}^{2+}$  та побудовано низькочастотні спектри КРС. У діапазоні спектра близько  $150 \text{ cm}^{-1}$  знайдено нову моду іон-фосфатних коливань, що характеризує коливання протиіонів  $\text{Mg}^{2+}$ . Результати розрахунків показали, що інтенсивності мод коливань Z-ДНК є чутливими до концентрації протиіонів магнію. Одержані результати добре описують експериментальні спектри КРС Z-ДНК.